NACA RM L57F25

NACA

RESEARCH MEMORANDUM

EFFECT OF NOSE SHAPE ON SUBSONIC AERODYNAMIC CHARACTERISTICS OF A BODY OF REVOLUTION HAVING A FINENESS RATIO OF 10.94

By Edward C. Polhamus

Langley Aeronautical Laboratory
Langley Field, Va.

NATIONAL ADVISORY COMMITTEE
FOR AERONAUTICS

WASHINGTON

August 12, 1957
Declassified June 24, 1958

NATIONAL ADVISORY COMMITTEE FOR AERONAUTICS

RESEARCH MEMORANDUM

EFFECT OF NOSE SHAPE ON SUBSONIC AERODYNAMIC CHARACTERISTICS OF A BODY OF REVOLUTION HAVING A FINENESS RATIO OF 10.94

By Edward C. Polhamus

SUMMARY

The effect of nose shape on the normal-force, pitching-moment, and axial-force coefficients of a body of revolution having a fineness ratio of 10.94 has been determined at subsonic speeds. Six different nose shapes which were investigated included flat-faced noses having various corner radii, a hemispherical nose, and two ogival noses. Results are presented for an angle-of-attack range up to 22° for Mach numbers from 0.40 to 0.90 and indicate that even a small radius results in a large reduction in axial force and a significant reduction in normal force. In order to expedite publication of this information only a brief analysis of the data is made.

INTRODUCTION

The increasing interest in flight of aircraft and missiles at high supersonic speeds, where aerodynamic heating poses a severe problem, has to some extent changed the emphasis in the selection of the body nose shape. From a performance standpoint slender pointed noses are desirable since they reduce the forebody drag. However, since these shapes have extremely high heat-transfer rates and little capacity for absorbing heat, a considerable amount of interest in blunt noses which have lower heat-transfer rates and more volume for absorbing heat has developed in recent years. (See refs. 1 and 2, for example.) In addition to the heat-transfer benefits, blunt noses are desirable because of the optical requirements of various seeker systems, and hemispherical noses have generated considerable interest from both standpoints. However, recent tests in a Mach number 2 air jet having a stagnation temperature of approximately 4,000° F (ref. 3) have indicated that the general level of the aerodynamic heating on a flat face is about one-half that on a hemisphere. These results are in qualitative agreement with the theoretical trends noted in reference 4. Subsequent heat-transfer tests (ref. 5) on

truncated conical noses indicated that a certain amount of rounding at the corners is beneficial in reducing the heat transfer on the conical portion of the nose. In view of these findings and the general interest in blunt noses it was felt that information on the effect of nose shape on the aerodynamic characteristics of a body of revolution having a relatively high fineness ratio would be desirable. A search of the literature indicated that, whereas considerable research has been conducted on the general effect of nose shape on bodies of revolution having high fineness ratios (see refs. 6 to 13, for example), no systematic studies of the effect of corner modifications to flat-faced noses appears to be available for these bodies.

The purpose of the present investigation, therefore, was to determine the effect of nose shape on the subsonic aerodynamic characteristics of a body of revolution having a high fineness ratio. The body had an overall fineness ratio of 10.94 and was tested with six different nose shapes including flat-faced noses having various corner radii, a hemispherical nose, and two ogival noses. Normal-force, pitching-moment, and axial-force coefficients were obtained at angles of attack ranging from -2° to 22° in the Mach number range from 0.40 to 0.90. In order to expedite publication of this information only a brief analysis of the data is made.

COEFFICIENTS AND SYMBOLS

The data are presented relative to the body axis system and the positive direction of the forces, moment, and angle of attack is shown in figure 1. The origin of the axis system is located at 57 percent of the overall length rearward of the nose. The various symbols used throughout the paper are defined as follows:

C_A axial-force coefficient (corrected to condition of free-stream static pressure at base), $\frac{\text{Axial force}}{qS}$

C_m pitching-moment coefficient, $\frac{\text{Pitching moment}}{qSD}$

C_N normal-force coefficient, $\frac{\text{Normal force}}{qS}$

D base diameter of body, ft unless otherwise noted

l body length, ft

M	Mach number
q	free-stream dynamic pressure, $\rho V^2/2$, lb/sq ft
R	Reynolds number, $\frac{\rho V l}{\mu}$
r	radius of fuselage nose, ft unless otherwise noted
S	base area of body, $\frac{\pi D^2}{4}$, sq ft
V	free-stream velocity, ft/sec
α	angle of attack, deg
μ	viscosity of air, slugs/ft-sec
ρ	air density, slugs/cu ft

MODELS AND TEST EQUIPMENT

Details of the various bodies tested are presented in figure 2. The top sketch shows the overall length, the maximum diameter, the moment reference point, and the length of the removable nose section, all of which are common to the various bodies tested. All the bodies had a fineness ratio of 10.94 and were cylindrical except for various portions of the removable nose. The two sketches at the bottom are enlarged views of the removable nose section and show the various nose configurations investigated. The center sketch shows the four nose radii ranging from 0 (blunt nose) to 2.50 inches (hemispherical nose) while the lower sketch shows the two ogival noses investigated.

The tests were conducted in the Langley high-speed 7- by 10-foot tunnel, and the models were mounted on a sting support system which can be remotely operated through an angle-of-attack range. The aerodynamic forces and moments were determined by means of an internally mounted six-component strain-gage balance.

TESTS AND CORRECTIONS

The tests were conducted at free-stream Mach numbers of 0.40, 0.60, 0.80, and 0.90 through an angle-of-attack range from approximately -2° to 22°. The variation of test Reynolds number, based on overall body length, with test Mach number is presented in figure 3.

Jet-boundary corrections are negligible and therefore have not been applied. However, a small blockage correction as determined by the method of reference 14 has been applied to the Mach number and dynamic pressure. The axial force has been corrected for the buoyancy caused by the static-pressure gradient existing in the clear tunnel and in addition has been adjusted to the condition of free-stream static pressure at the base. The angle of attack has been corrected for the deflection of the sting support and the strain-gage balance under load.

RESULTS AND DISCUSSION

The basic data for the various nose shapes are presented in figures 4, 5, and 6 where the force and moment coefficients are presented as functions of angle of attack for various Mach numbers. Inasmuch as the axial-force coefficient exhibits the greatest variation with Mach number, the axial-force coefficient at zero angle of attack has been obtained over a more complete range of Mach number and the results are presented in figure 7. In figure 7 the flagged symbols represent the data obtained from figure 6. Since all of the bodies tested were of the same diameter and the wind tunnel used in the experiments does not permit control of the pressure, there was no opportunity to evaluate possible effects of Reynolds number at constant Mach number. Past experience has indicated that results on axial force at zero angle of attack, such as those summarized in figure 7, are determined more by Mach number than by Reynolds number. Characteristics at angle of attack, however, may be significantly influenced by the Reynolds number. For example, the abrupt increase in axial force shown in figure 6(b) for the body with a nose radius of 0.50 inch at $M = 0.40$ may be dependent upon Reynolds number.

In order to expedite publication of this information only a very limited analysis of the data has been made. However, a few interesting observations can be made with the aid of figures 7 and 8. In figure 7 it can be noted that even a small radius results in a large reduction in axial force due to the reduction in forebody drag, and that at low Mach numbers additional nose modifications have relatively little effect. At the higher Mach numbers supercritical velocities are encountered and a more gradual variation of axial force with nose radius, or nose fineness ratio, exists.

In order to show better the effect of nose shape and Mach number on the normal force, figure 8 has been prepared. In figure 8(a) the normal-force coefficient at a Mach number of 0.60 is plotted as a function of the nondimensional nose radius r/D for angles of attack of 10°, 15°, and 20°. In order to show more clearly the large effect in the small-radius range, a logarithmic scale has been used and it should be noted

that the values for zero radius have been plotted at $r/D = 0.01$. The rather large effects of nose shape that exist in the blunt range of shapes are clearly evident. For example, at an angle of attack of 20° as the shape changes from the hemisphere ($r/D = 0.50$) to the blunt nose the normal force increases by approximately 28 percent, whereas a change from the high-fineness-ratio ogive ($r/D = 12.5$) to the hemisphere resulted in only a 9-percent increase.

In figure 8(b) the normal-force coefficient is presented as a function of Mach number for two of the nose shapes at an angle of attack of 20°. The results which are presented for the flat-faced nose and the long ogival nose indicate an appreciable increase in normal-force coefficient with Mach number.

Langley Aeronautical Laboratory,
National Advisory Committee for Aeronautics,
Langley Field, Va., June 7, 1957.

REFERENCES

1. Allen, H. Julian, and Eggers, A. J., Jr.: A Study of the Motion and Aerodynamic Heating of Missiles Entering the Earth's Atmosphere at High Supersonic Speeds. NACA RM A53D28, 1953.

2. Sibulkin, M.: Heat Transfer Near the Forward Stagnation Point of a Body of Revolution. Jour. Aero. Sci. (Readers' Forum), vol. 19, no. 8, Aug. 1952, pp. 570-571.

3. Purser, Paul E., and Hopko, Russell N.: Exploratory Materials and Missile-Nose-Shape Tests in a 4,000° F Supersonic Air Jet. NACA RM L56J09, 1956.

4. Van Driest, E. R.: The Problem of Aerodynamic Heating. Rep. No. AL-2303, North American Aviation, Inc., May 1, 1956.

5. Carter, Howard S., and Bressette, Walter E.: Heat Transfer and Pressure Distribution on Six Blunt Noses at a Mach Number of 2. NACA RM L57C18, 1957.

6. Wallskog, Harvey A., and Hart, Roger G.: Investigation of the Drag of Blunt-Nosed Bodies of Revolution in Free Flight at Mach Numbers From 0.6 to 2.3. NACA RM L53D14a, 1953.

7. Piland, Robert O., and Putland, Leonard W.: Zero-Lift Drag of Several Conical and Blunt Nose Shapes Obtained in Free Flight at Mach Numbers of 0.7 to 1.3. NACA RM L54A27, 1954.

8. Gapcynski, John P., and Robins, A. Warner: The Effect of Nose Radius and Shape on the Aerodynamic Characteristics of a Fuselage and a Wing-Fuselage Combination at Angles of Attack. NACA RM L53I23a, 1953.

9. Sommer, Simon C., and Stark, James A.: The Effect of Bluntness on the Drag of Spherical-Tipped Truncated Cones of Fineness Ratio 3 at Mach Numbers 1.2 to 7.4. NACA RM A52B13, 1952.

10. Seiff, Alvin, Sandahl, Carl A., Chapman, Dean R., Perkins, E. W., and Gowen, F. E.: Aerodynamic Characteristics of Bodies at Supersonic Speeds. A Collection of Three Papers. NACA RM A51J25, 1951.

11. Walchner, O.: Systematic Wind-Tunnel Measurements on Missiles. NACA TM 1122, 1947.

12. Jaeger, B. F., and deLancy, L. M.: The Aerodynamic Characteristics at Mach Number 1.57 of 10-, 14-, and 18-Caliber Cylindrical Bare Bodies With Varying Head Shapes. NAVORD Rep. 1922 (NOTS 450), U. S. Naval Ord. Test Station, Inyokern (China Lake, Calif.), Oct. 31, 1951.

13. Hahn, H. J.: Windkanalmessungen an Geschossformen mit verschieden langen Spitzen. (Wind-Tunnel Measurements on Missile Forms With Points of Various Lengths.) Bericht AVA 8/17/39, Aerodynamische Versuchsanstalt Göttingen, Nov. 20, 1939.

14. Herriot, John G.: Blockage Corrections for Three-Dimensional-Flow Closed-Throat Wind Tunnels, With Consideration of the Effect of Compressibility. NACA Rep. 995, 1950. (Supersedes NACA RM A7B28.)

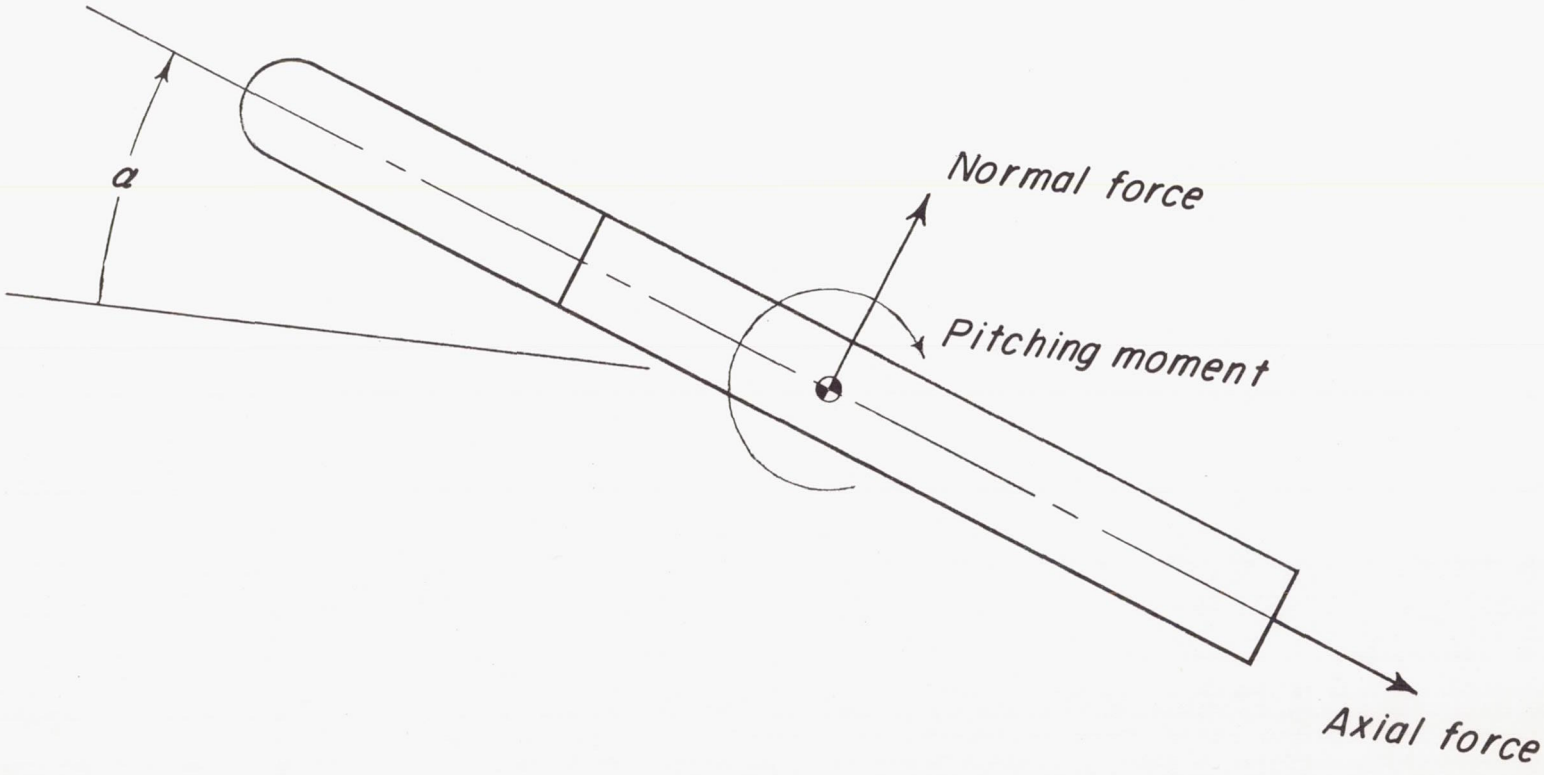

Figure 1.- Body reference axis showing positive direction of forces, moment, and angle of attack.

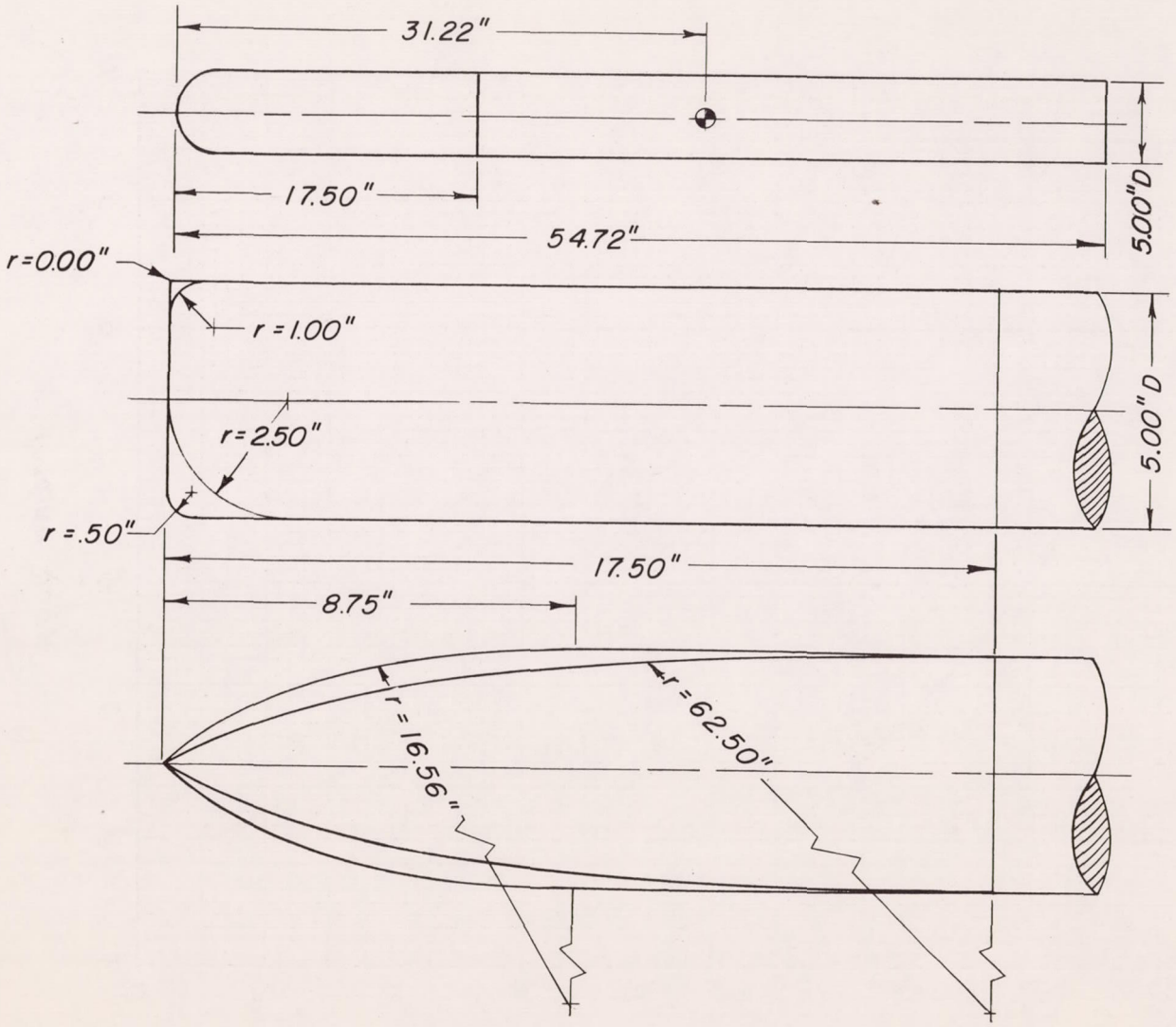

Figure 2.- Sketch of various nose shapes tested with values of the radii indicated for the six nose shapes.

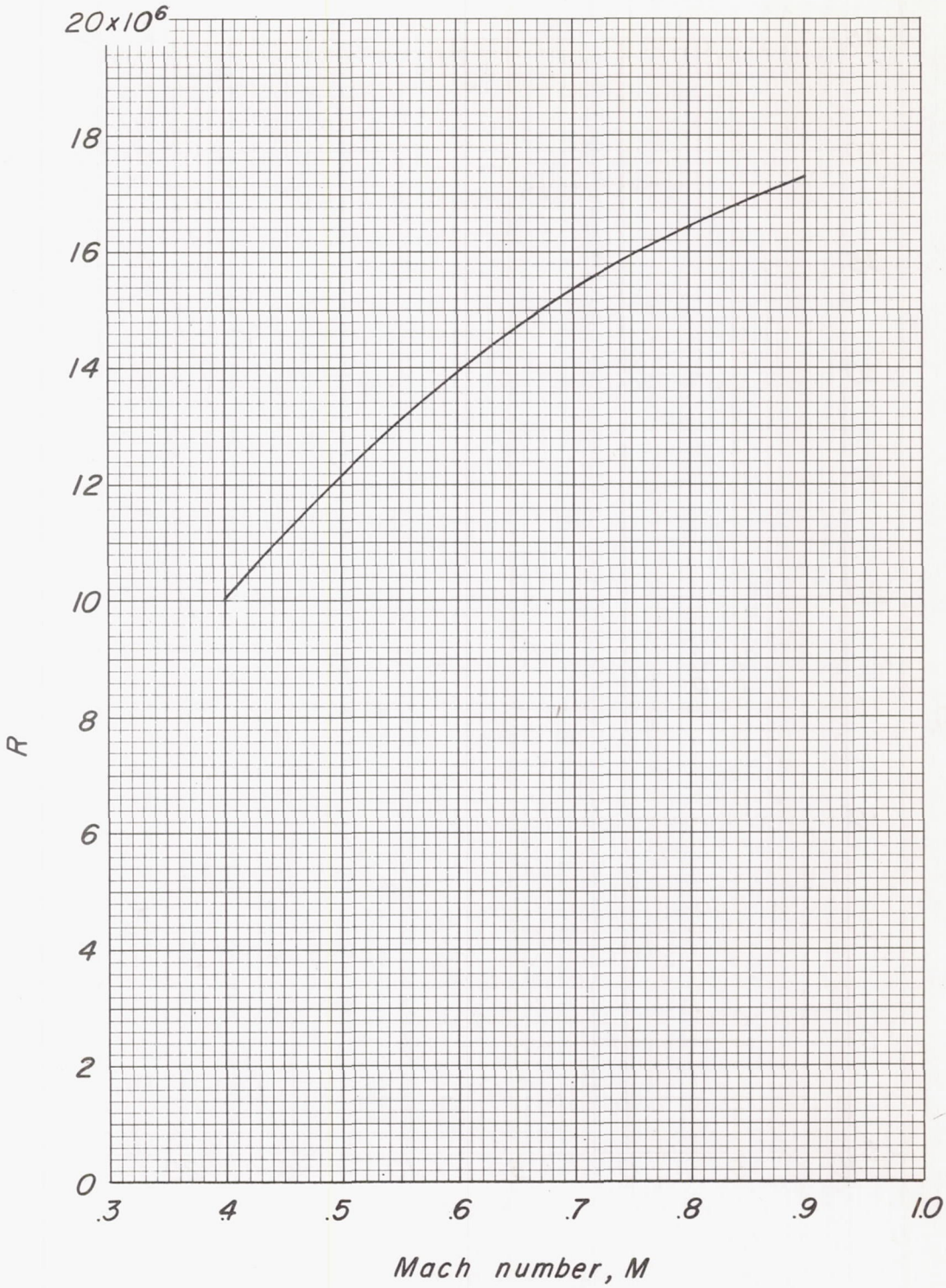

Figure 3.- Variation of Reynolds number with Mach number.

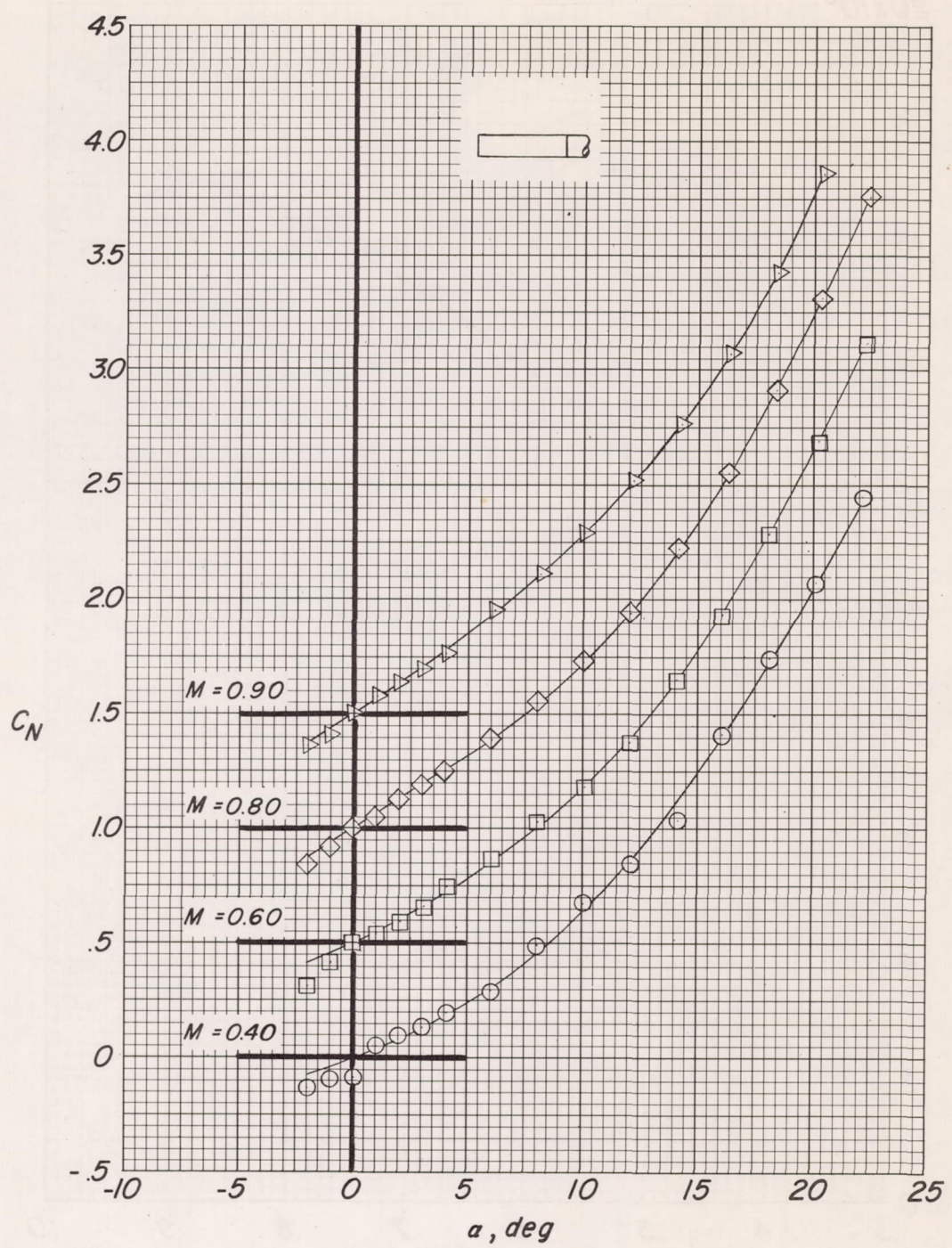

(a) r = 0.00 inch.

Figure 4.- Variation of C_N with angle of attack.

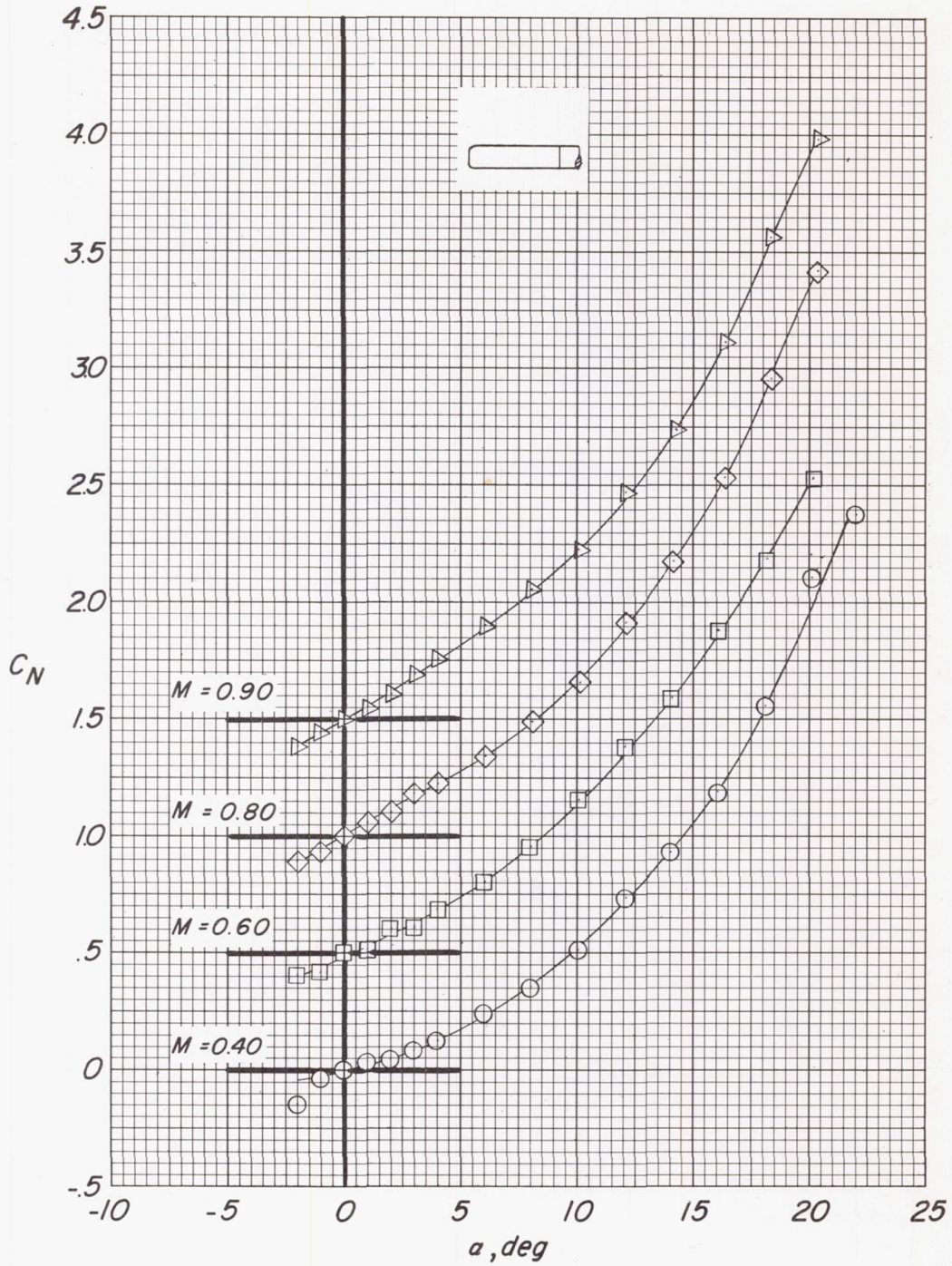

(b) r = 0.50 inch.

Figure 4.- Continued.

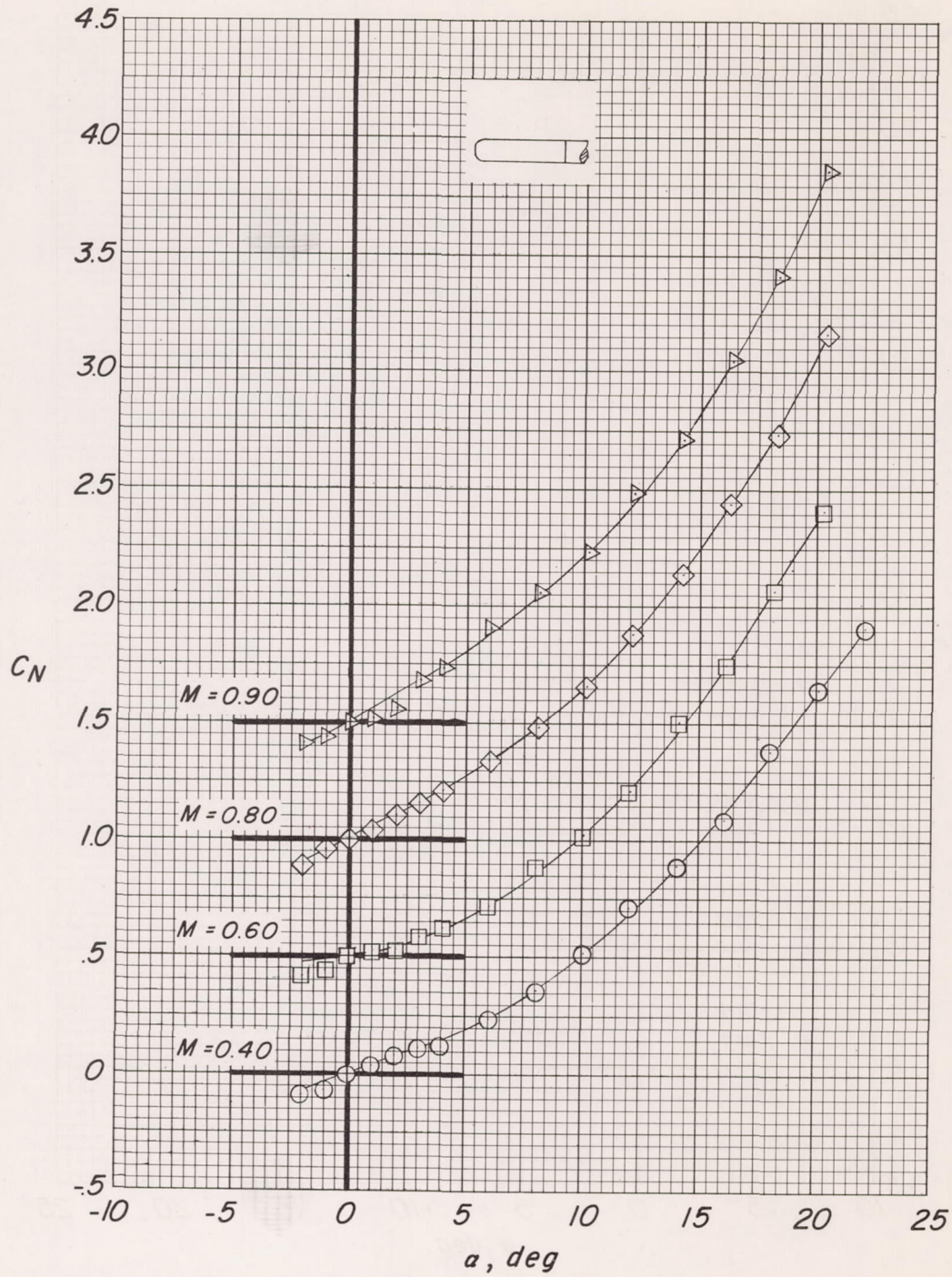

(c) r = 1.00 inch.

Figure 4.- Continued.

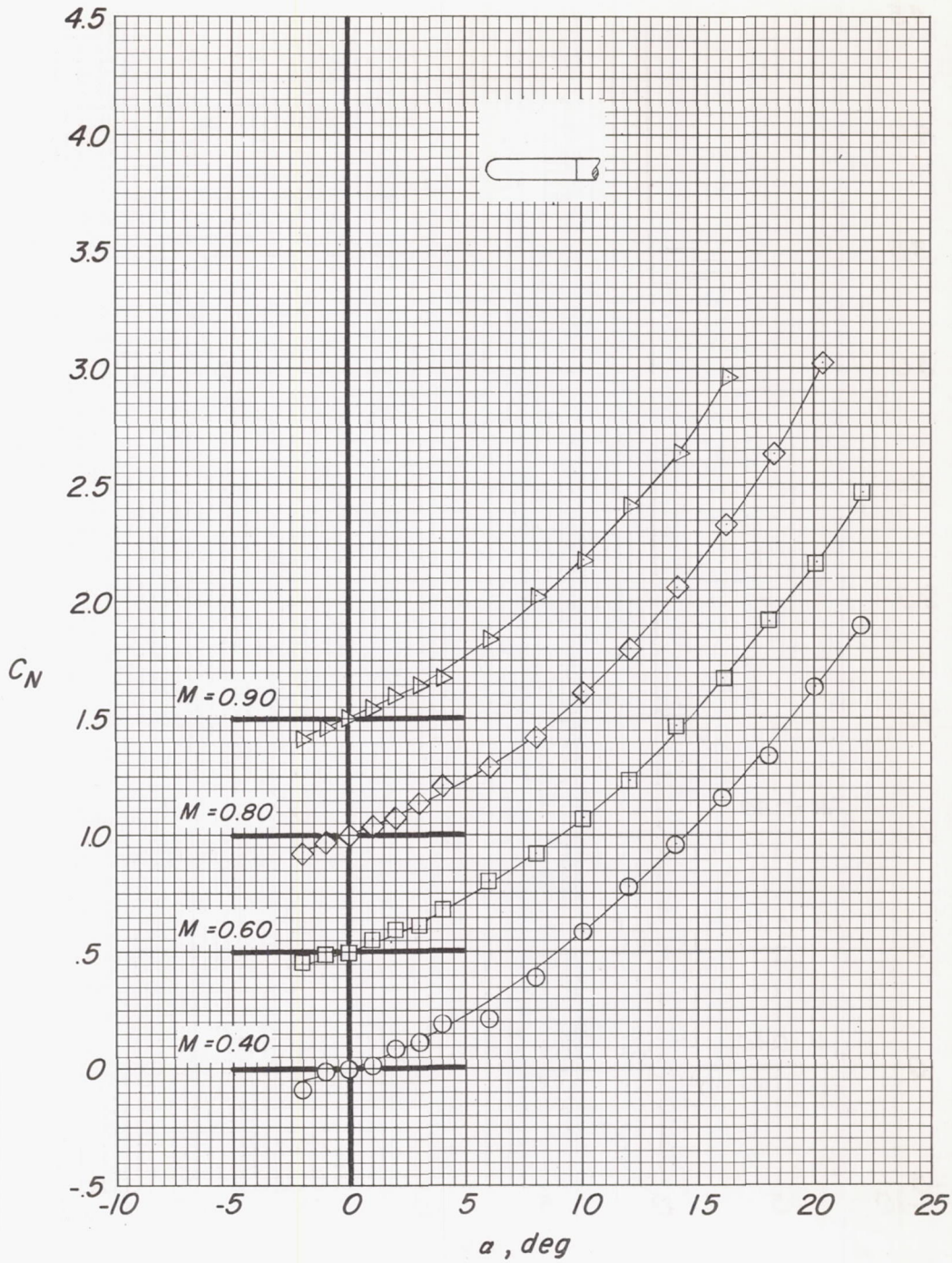

(d) r = 2.50 inches.

Figure 4.- Continued.

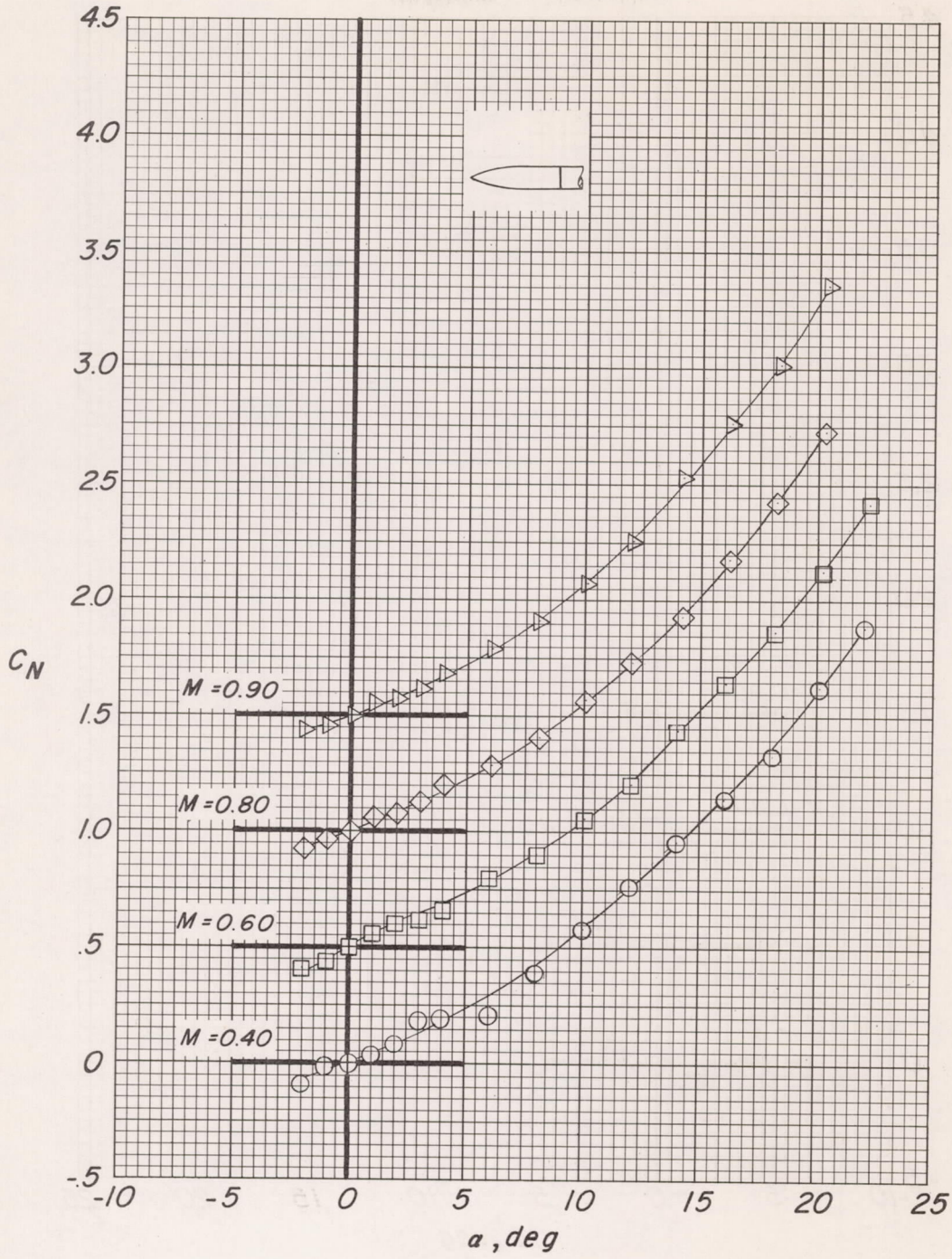

(e) r = 16.56 inches.

Figure 4.- Continued.

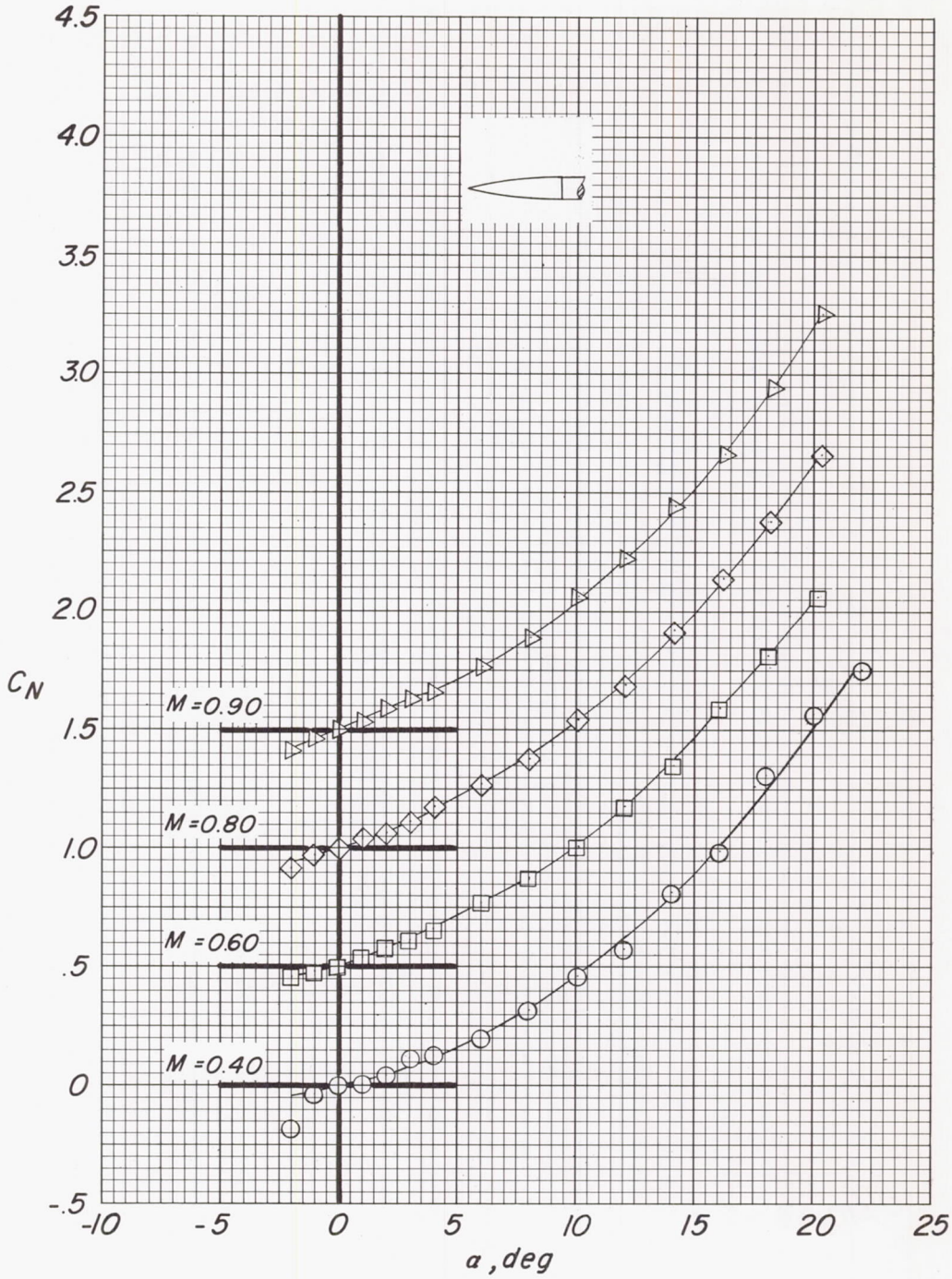

(f) r = 62.50 inches.

Figure 4.- Concluded.

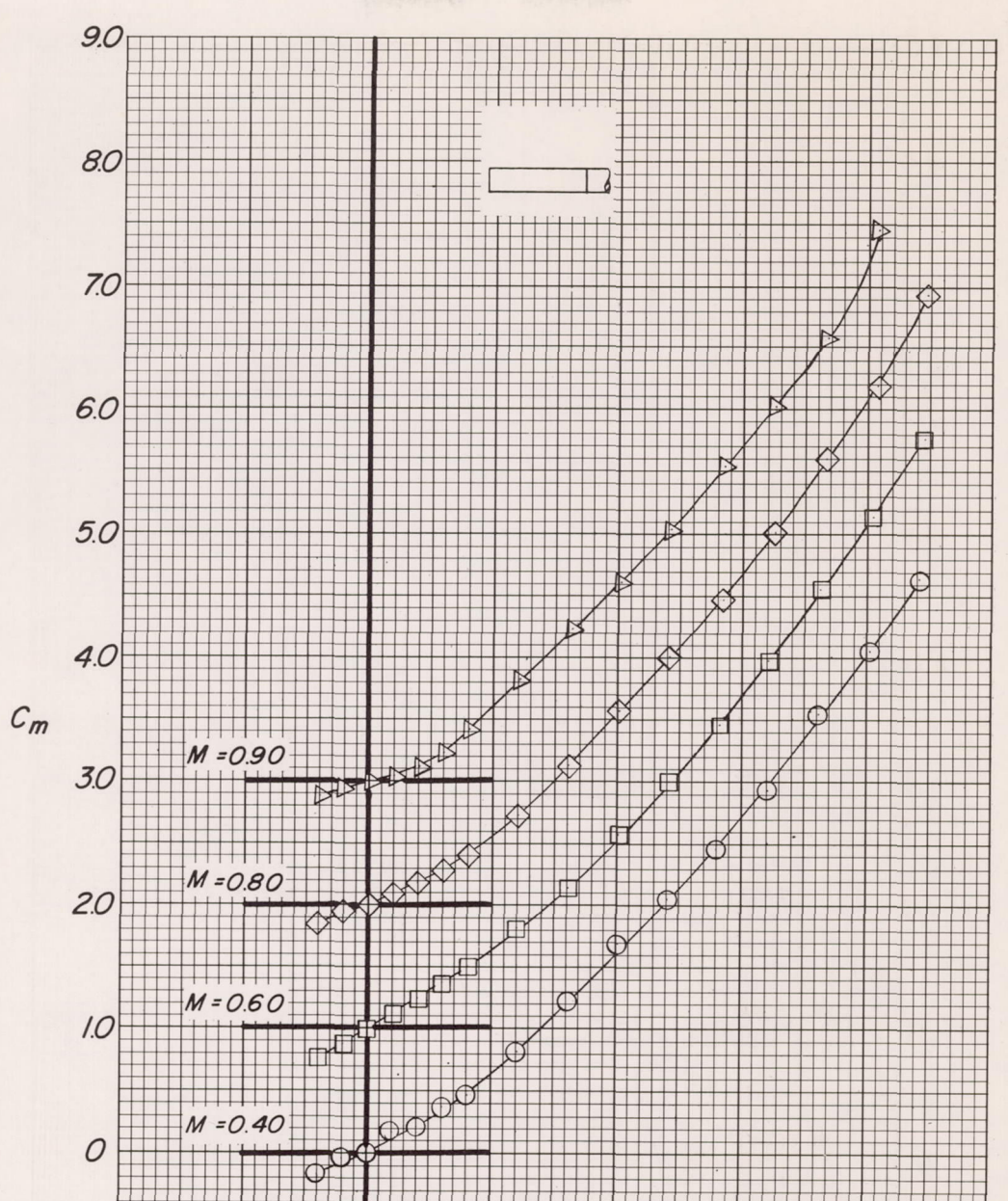

(a) r = 0.00 inch.

Figure 5.- Variation of C_M with angle of attack.

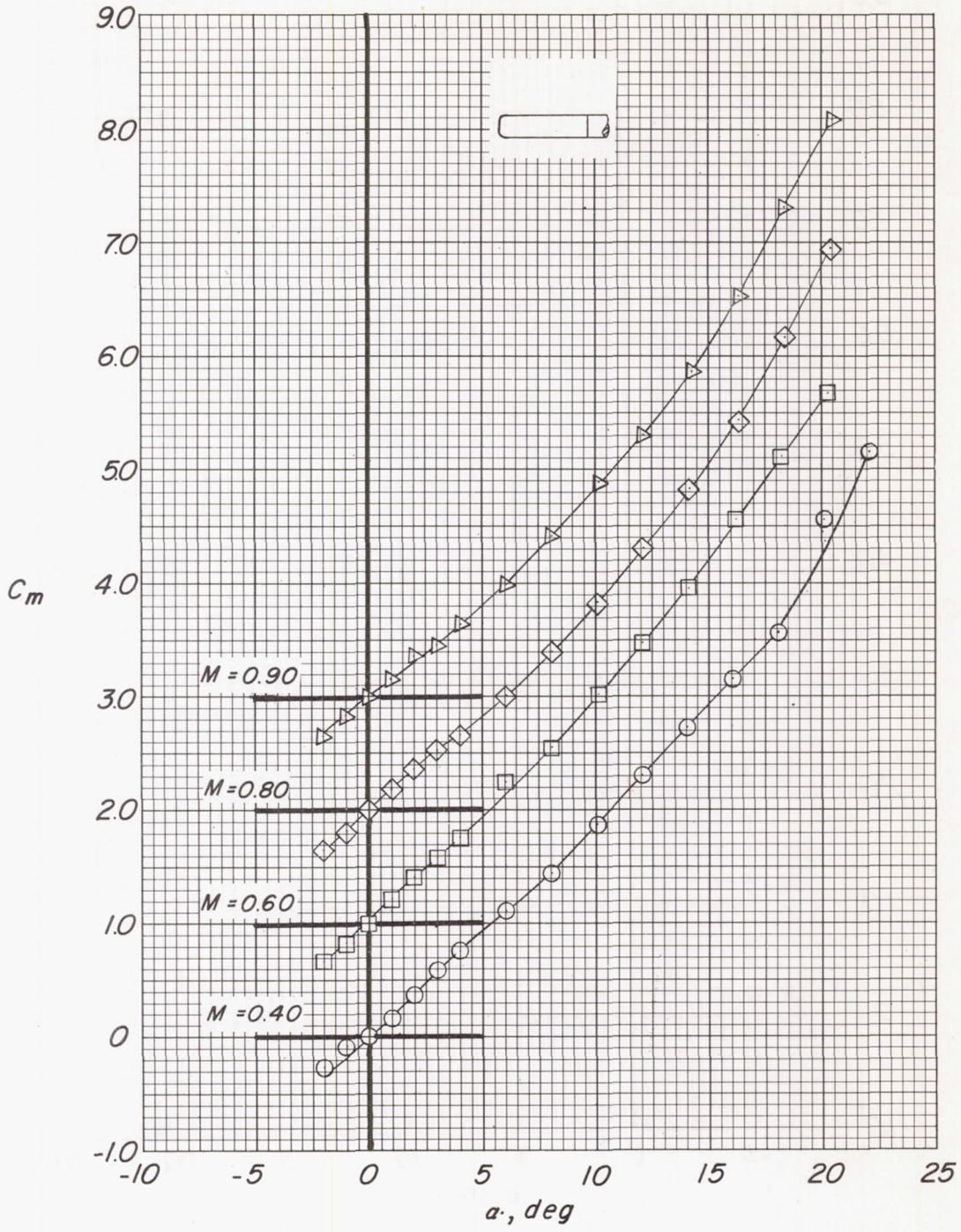

(b) r = 0.50 inch.

Figure 5.- Continued.

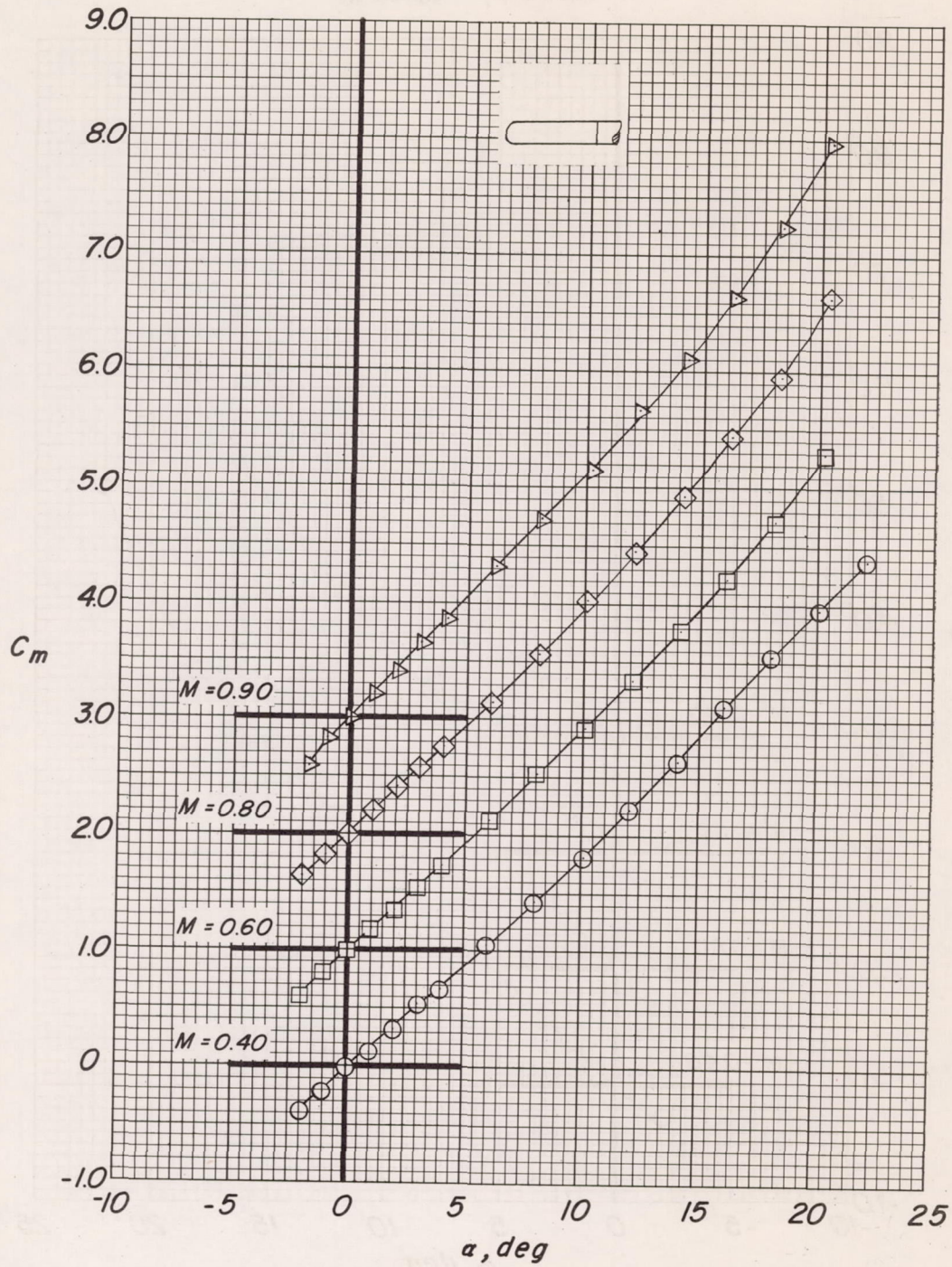

(c) r = 1.00 inch.

Figure 5.- Continued.

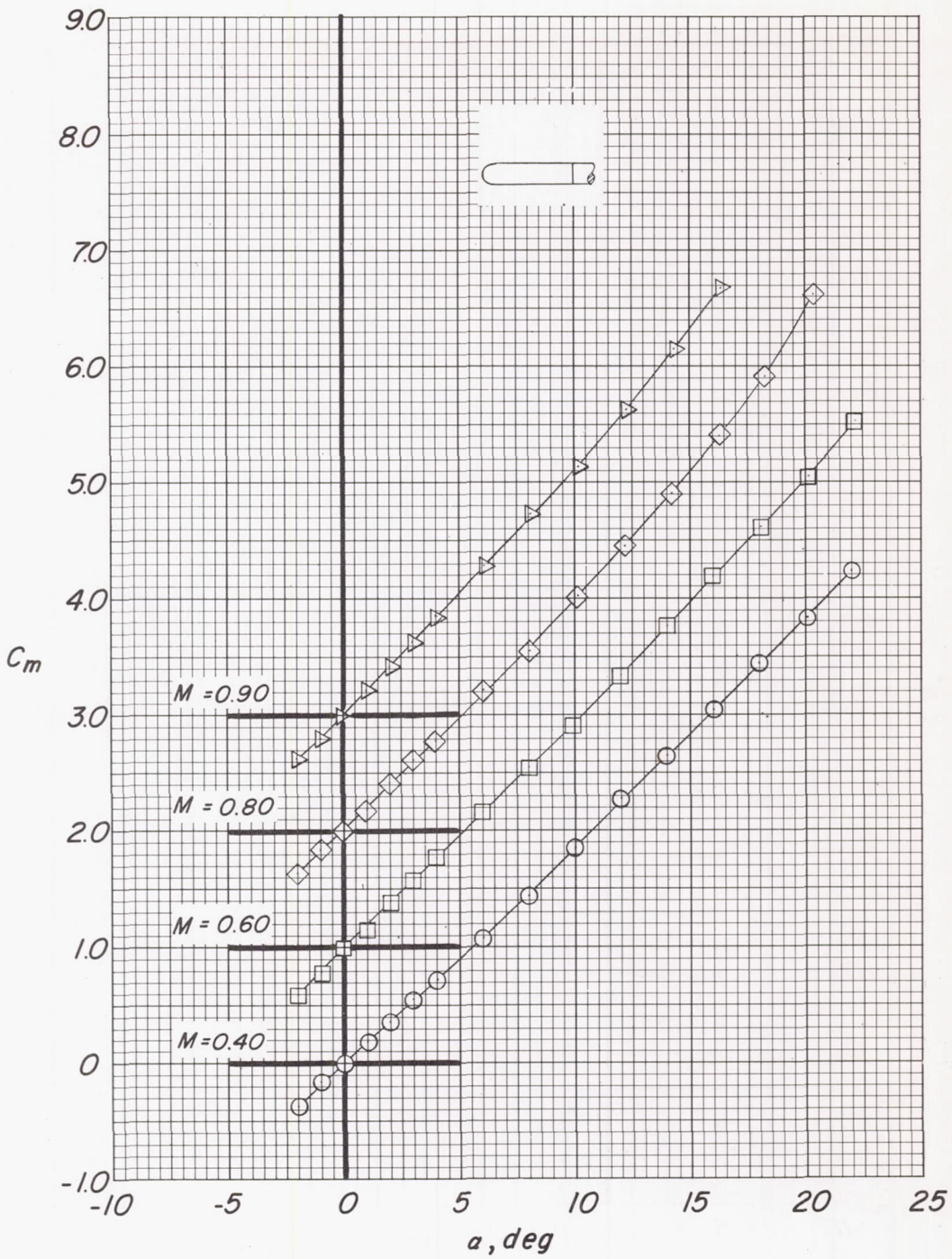

(d) r = 2.50 inches.

Figure 5.- Continued.

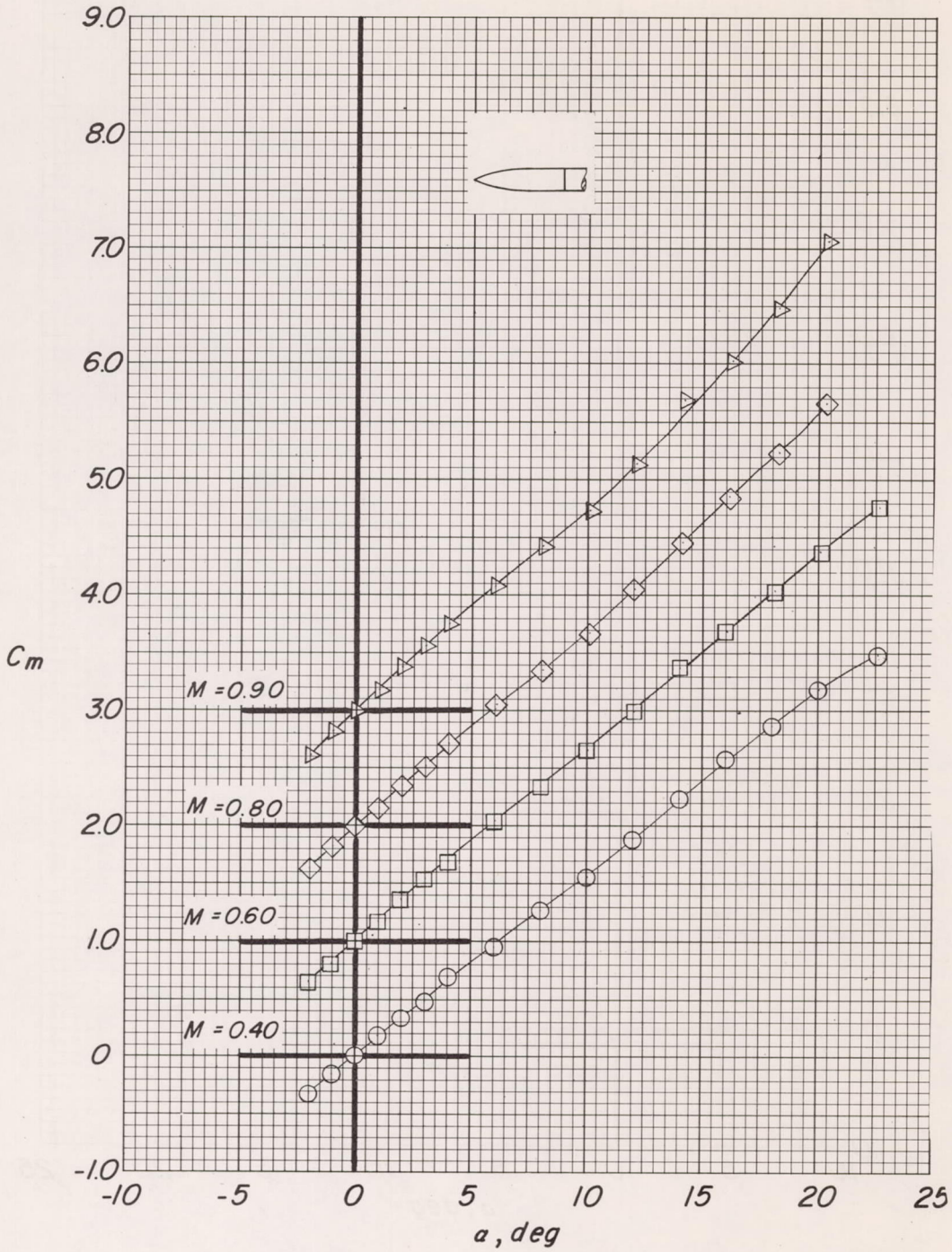

(e) r = 16.56 inches.

Figure 5.- Continued.

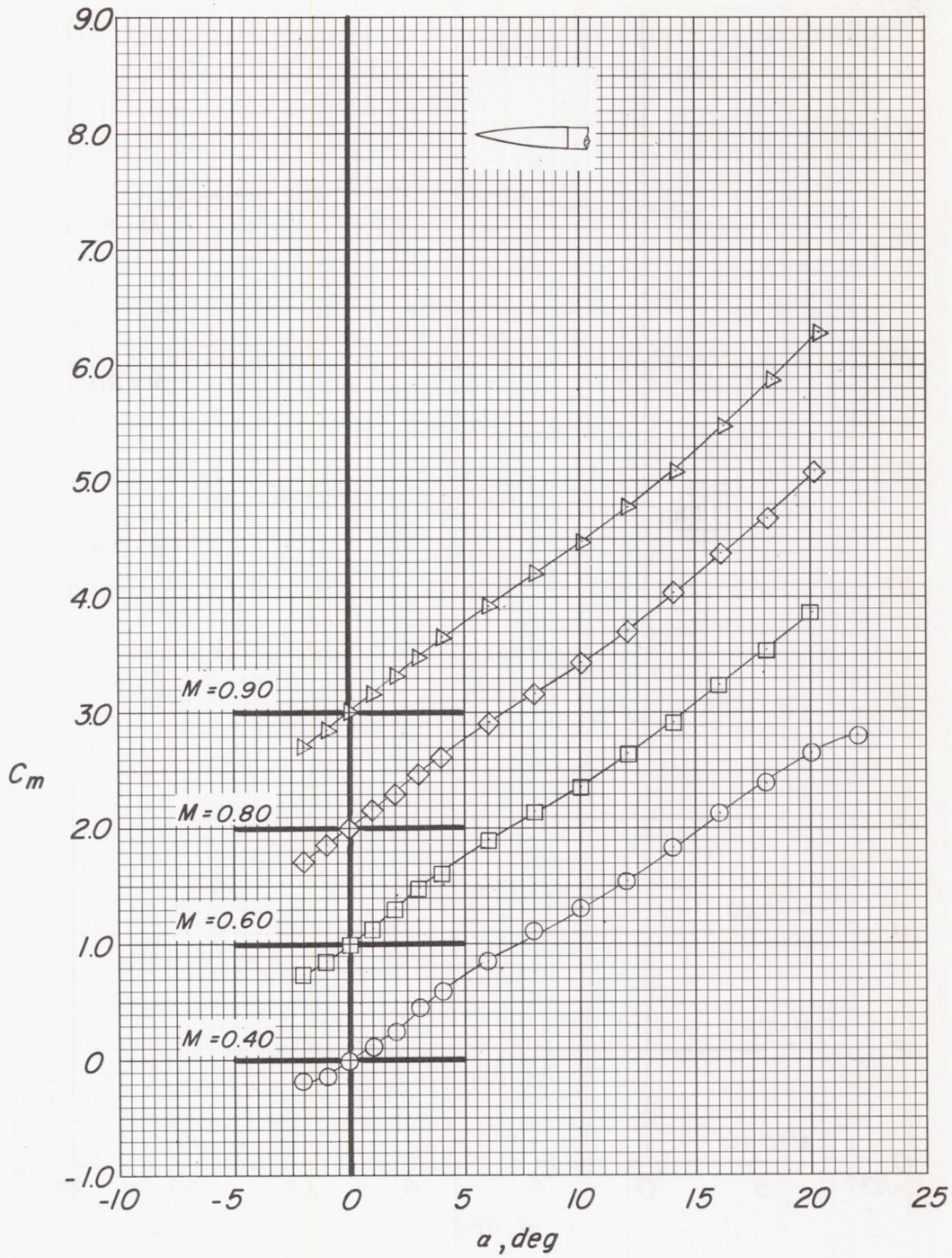

(f) r = 62.50 inches.

Figure 5.- Concluded.

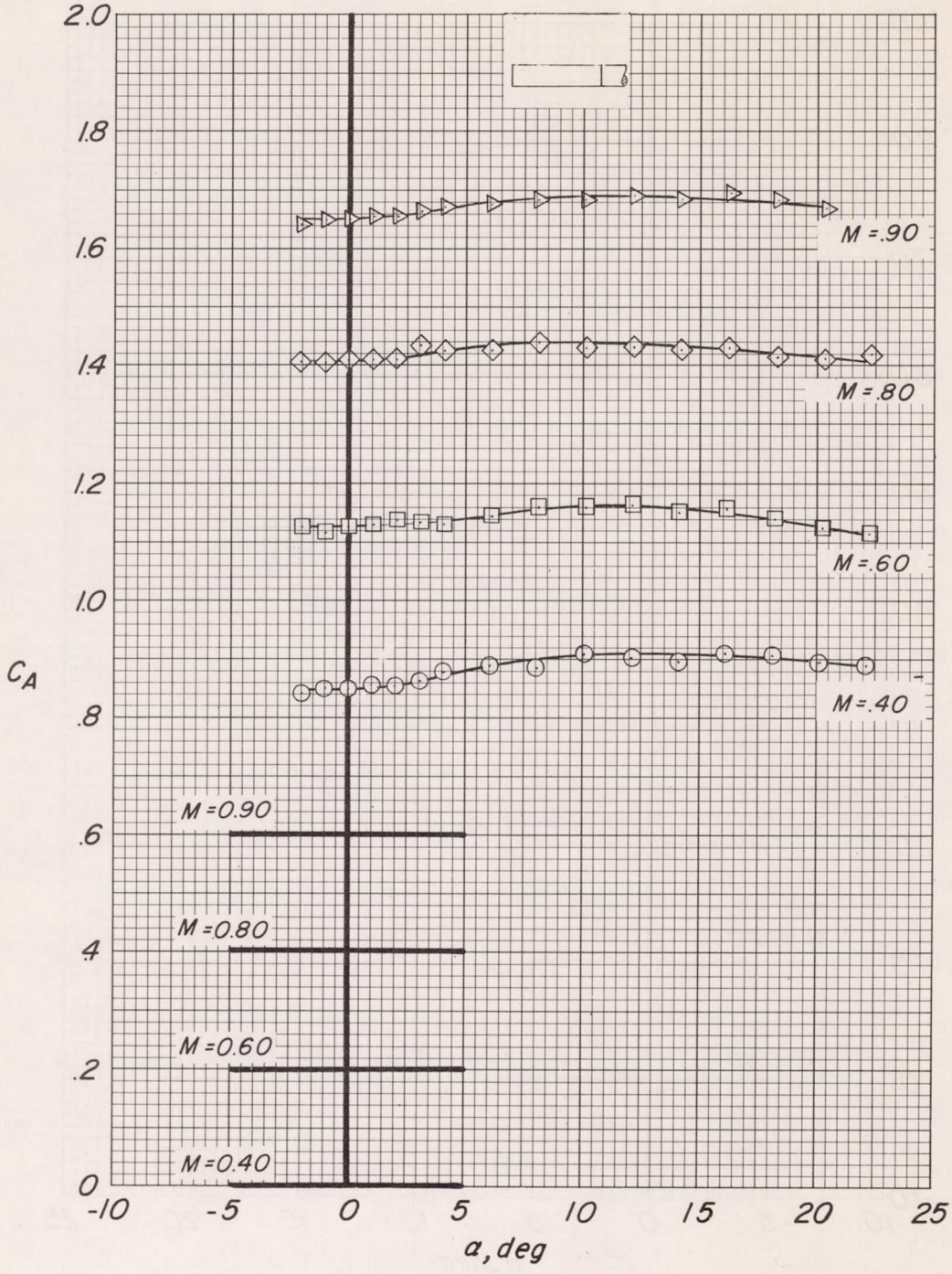

(a) r = 0.00 inch.

Figure 6.- Variation of C_A with angle of attack.

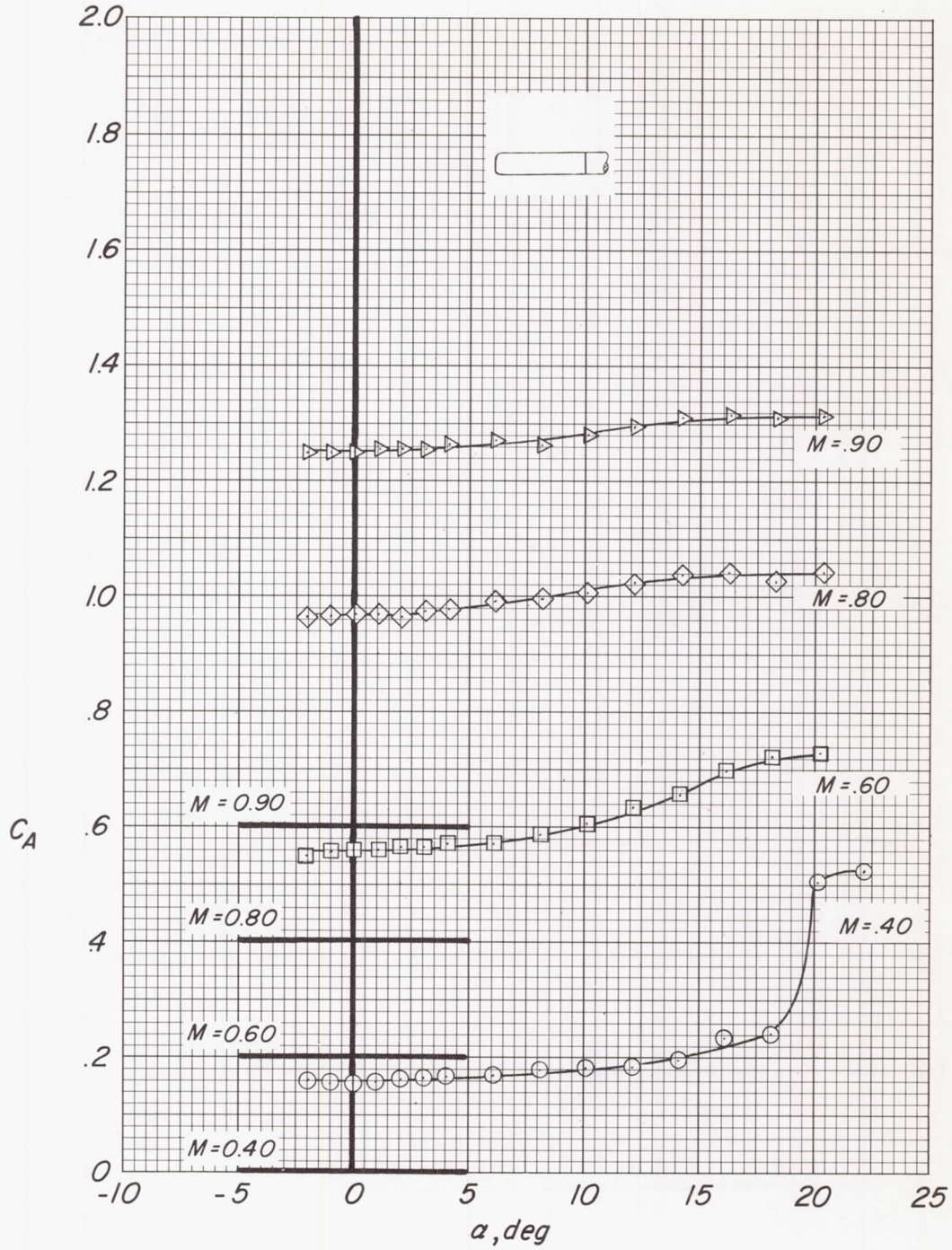

(b) r = 0.50 inch.

Figure 6.- Continued.

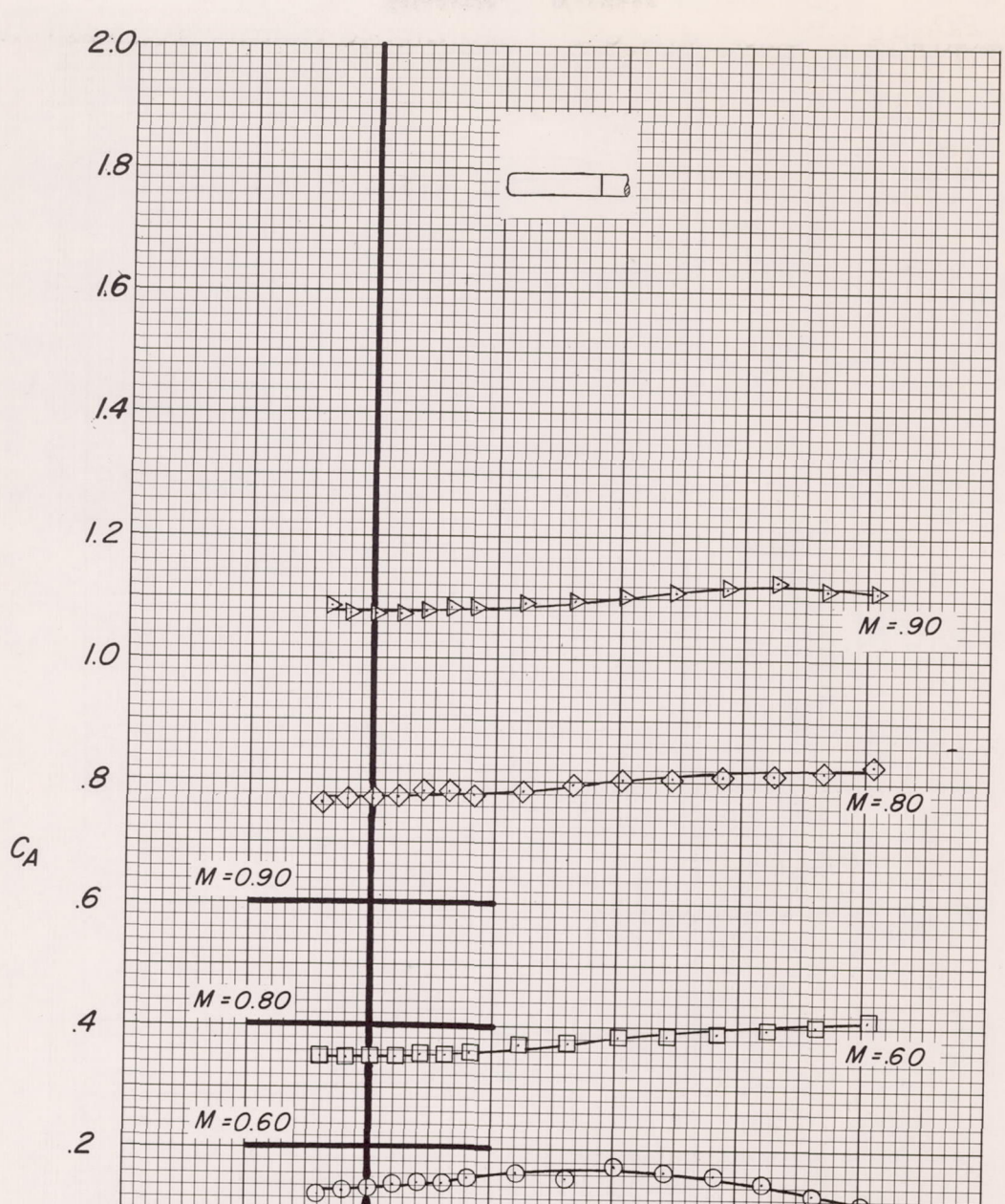

(c) r = 1.00 inch.

Figure 6.- Continued.

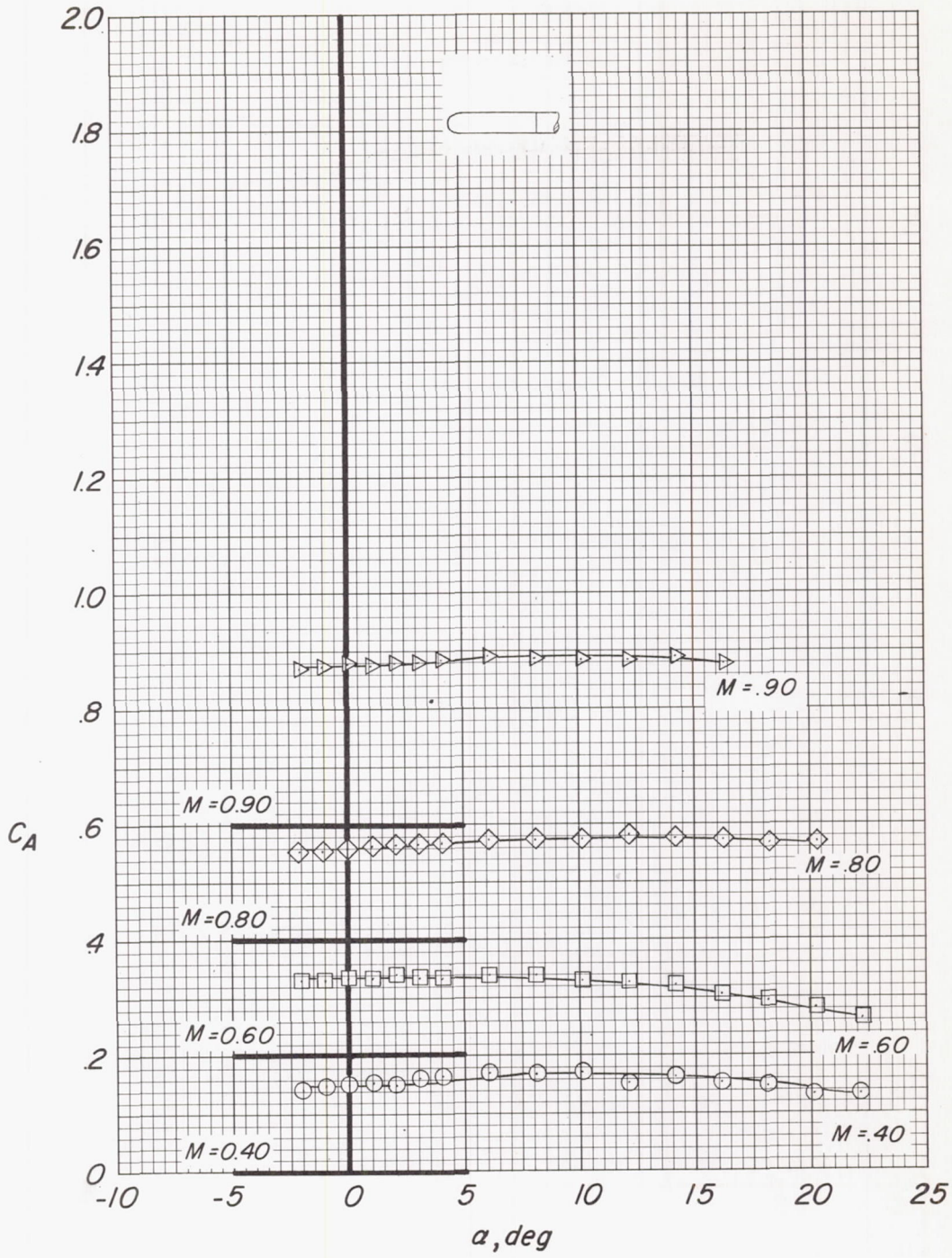

(d) r = 2.50 inches.

Figure 6.- Continued.

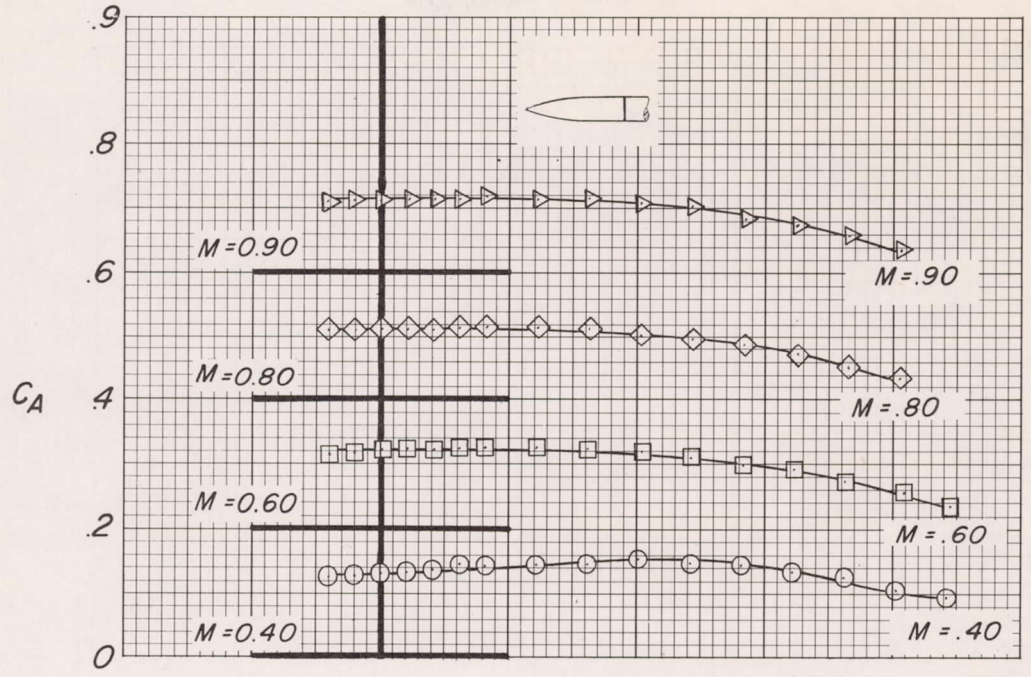

(e) r = 16.56 inches.

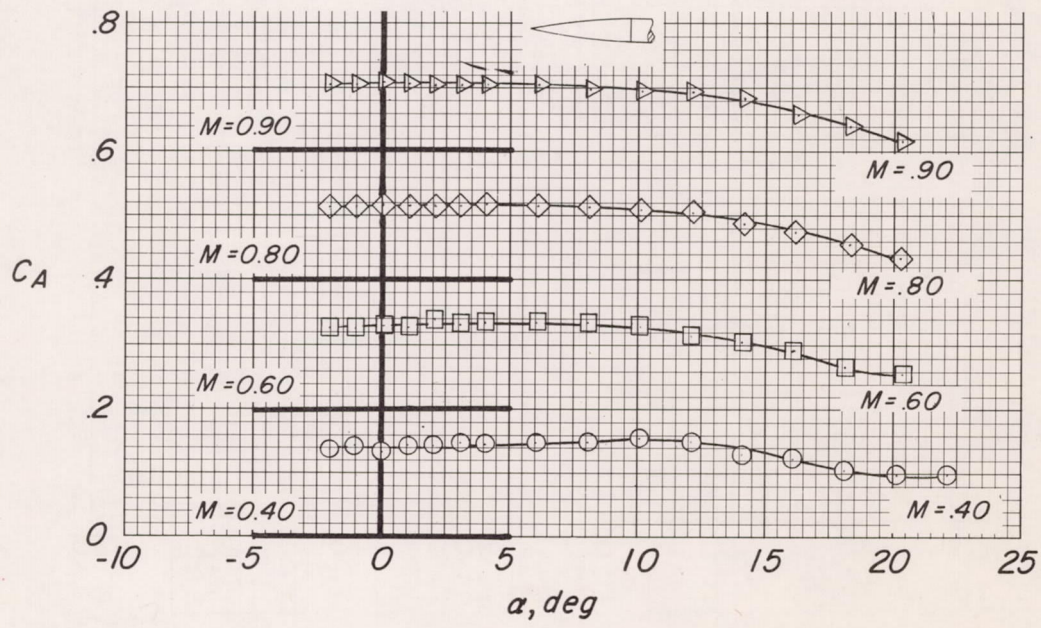

(f) r = 62.50 inches.

Figure 6.- Concluded.

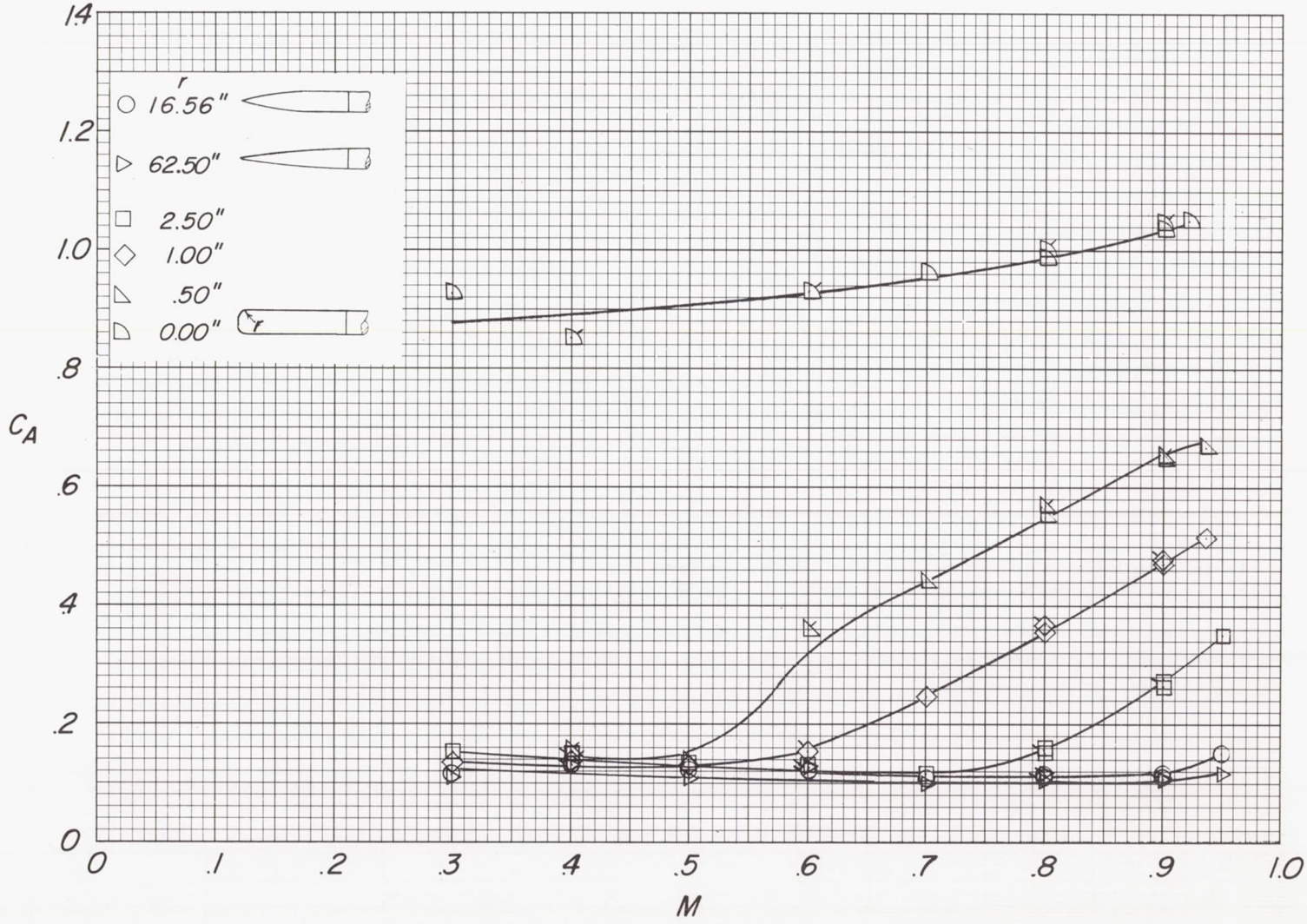

Figure 7.- Effect of nose shape on variation of C_A with Mach number. $\alpha = 0^\circ$.

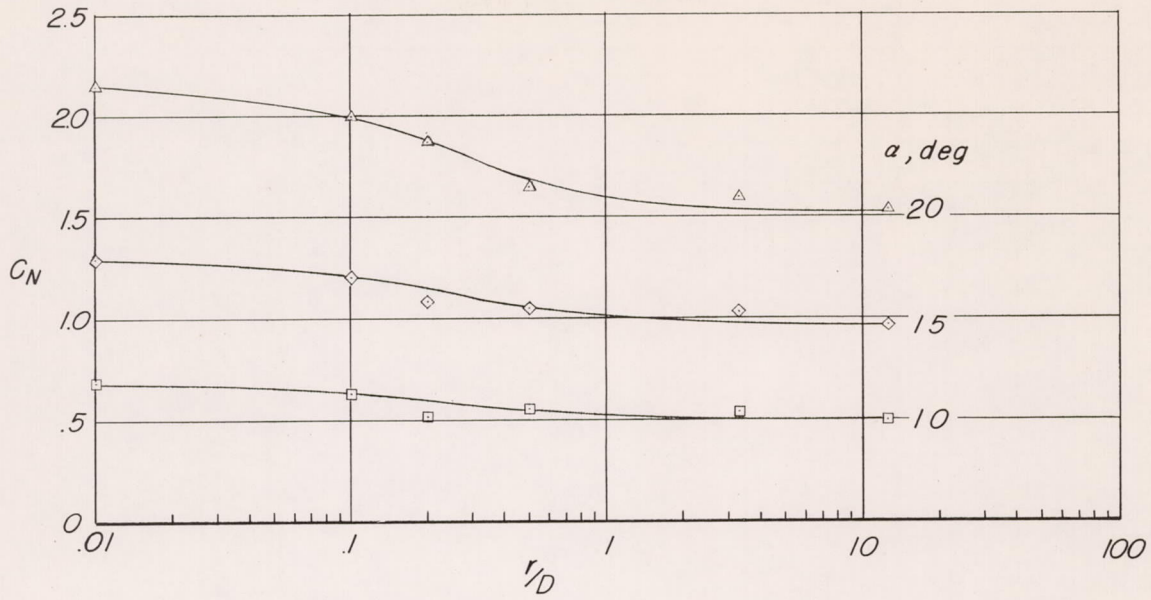

(a) Effect of nose radius. M = 0.60.

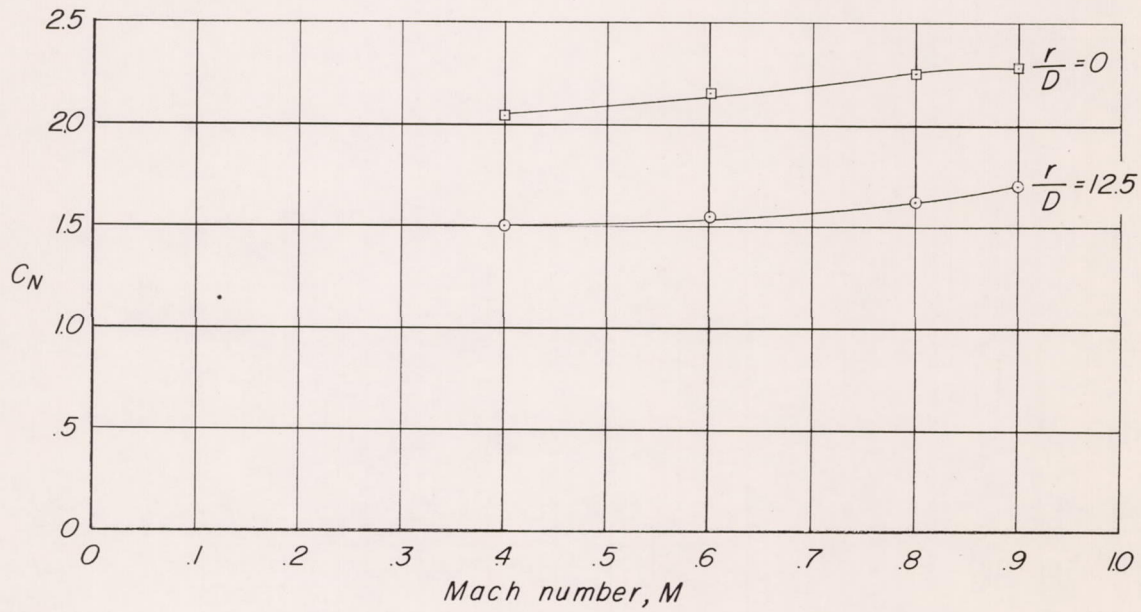

(b) Effect of Mach number. $\alpha = 20^\circ$.

Figure 8.- Effect of nose radius and Mach number on normal-force coefficient.